Theoretical Investigation of the Dynamics of the Active Site Lid in *Rhizomucor miehei* Lipase

Günther H. Peters,*# O. H. Olsen,# A. Svendsen,# and R. C. Wade§
*Chemistry Department III, H. C. Ørsted Institutet, University of Copenhagen, DK-2100 Copenhagen Ø, Denmark; #Novo-Nordisk A/S, DK-2880 Bagsvaerd, Denmark; and §European Molecular Biology Laboratory, D-6912 Heidelberg, Germany

ABSTRACT Interfacial activation of *Rhizomucor miehei* lipase is accompanied by a hinge-type motion of a single helix (residues 83–94) that acts as a lid over the active site. Activation of the enzyme involves the displacement of the lid to expose the active site, suggesting that the dynamics of the lid could be of mechanistic and kinetic importance. To investigate possible activation pathways and to elucidate the effect of a hydrophobic environment (as would be provided by a lipid membrane) on the lid opening, we have applied molecular dynamics and Brownian dynamics techniques. Our results indicate that the lipase activation is enhanced in a hydrophobic environment. In nonpolar low-dielectric surroundings, the lid opens in approximately 100 ns in the BD simulations. In polar high-dielectric (aqueous) surroundings, the lid does not always open up in simulations of up to 900 ns duration, but it does exhibit some gating motion, suggesting that the enzyme molecule may exist in a partially active form before the catalytic reaction. The activation is controlled by the charged residues ARG86 and ASP91. In the inactive conformation, ASP91 experiences repulsive forces and pushes the lid toward the open conformation. Upon activation ARG86 approaches ASP61, and in the active conformation, these residues form a salt bridge that stabilizes the open conformation.

INTRODUCTION

Lipases have been used as models for studying the regulation of interfacial enzyme-catalyzed reactions for many years. Considerable insight has been obtained from the crystal structures of several lipases (Derewenda et al., 1994; Brzozowski et al., 1991), including the inactive and active forms of the lipase-inhibitor complexes. The crystal structures indicate that the conformational changes during activation are rigid body hinge-type motions of single or multiple helices (Derewenda et al., 1994) (see Fig. 1). Here we restrict our discussion to a particular lipase, the *Rhizomucor miehei* lipase (Rml). Like many lipases, it has a catalytic center with a chymotrypsin-like triad [SER . . . HIS . . . ASP], which is shielded from the solvent by a helical loop, which is referred to in the literature as a "lid." During activation, the lid is displaced to allow access of the substrate to the active site. From the crystal structures, it is evident not only that the backbone of the central part of the lid moves by more than 7 Å, but also that the hydrophobic surface increases by approximately 750 $Å^2$ (U. Derewenda et al., 1992), which agrees well with the general observation that, in an aqueous solution, the lipase activity is increased in the presence of a lipid interface (Verger et al., 1984; Piéroni et al., 1990). The overall catalytic process involves adsorption of the enzyme from the bulk aqueous phase onto the lipid surface and catalysis at the interface (Derewenda et al., 1994; Brockman, 1984).

Many mechanisms have been proposed to explain the activation of lipases at a lipid-water interface, including an increase in substrate concentration at the interface, better orientation of the scissile ester bond, reduction in the water shell around the ester molecules in water, and a conformational change in the enzyme. Theoretical treatments of the catalytic process are based either on a surface-mediated mechanism (Derewenda et al., 1994; Thuren, 1988) ("substrate theory"), which suggests that the preexisting surface structure and/or different meso and crystalline phases of the lipid substrate may have considerable influence on the behavior of lipolytic enzymes, or on the conformational changes in the enzyme upon adsorption onto the interface ("enzyme theory") (Muderhwa and Brockman, 1992). These models are merely conceptual extremes and are not mutually exclusive. Our previous studies focused on studying the phases and interfacial properties of the lipid substrate (Peters et al., 1993, 1994, 1995a,b). Here, however, we will focus on aspects involving the enzyme.

Although progress has been achieved in our understanding of the relationship between different lipases, largely because of x-ray studies (Derewenda et al., 1994), there is still a gap in correlating the enzyme activity to the interfacial properties of the lipid substrate. X-ray diffraction data provide important but predominantly static information about lipase structures. In solution, the motion of the enzyme may be complex, and in particular, as the enzyme approaches the substrate, lipid-enzyme interactions may play an important role in the activation process. It is exactly this intermediate region of the activation pathway which, at the present time, cannot be probed by experiment, but about which computer simulations might provide essential information. The motion of flexible loops in enzymes is of considerable interest (Wade et al., 1993; Kempner, 1993;

Received for publication 17 January 1996 and in final form 2 April 1996.
Address reprint requests to Dr. G. H. Peters, H. C. Ørsted Institutet, Chemistry Department 3, University of Copenhagen, Universitetsparken 5, DK-2100 Copenhagen Ø, Denmark. Tel.: 45-35320236; Fax: 45-35320259; E-mail: ghp@st.ki.ku.dk.
© 1996 by the Biophysical Society
0006-3495/96/07/119/11 $2.00

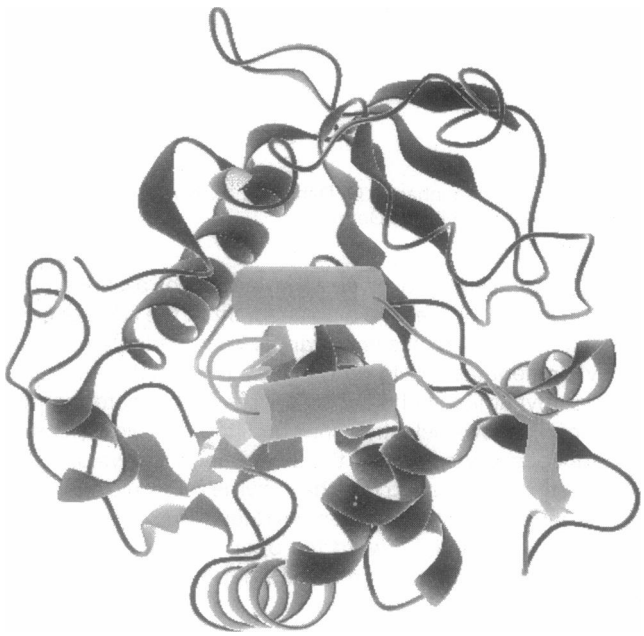

FIGURE 1 The Cα trace of *Rhizomucor miehei* lipase. The light grey regions show the conformations of the active site lid in the closed, ligand free (*lower*) and open (inhibitor-bound) (*upper*) crystal structures of Rml. The cylinders represent the helix in the active site lid.

Philippopoulos et al., 1995; Falzone et al., 1994; Williams and McDermott, 1995), because these structural changes may control biochemical activity. Thus, to establish a link between substrate properties and the lipase reaction, it is important to examine the dynamic motion of the lid over the active sites upon substrate binding.

We have applied two different simulation methods to probe different time scales. Molecular dynamics (MD) applied on the time scale of picoseconds and Brownian dynamics (BD) approaching the order of microseconds were used to study conformational changes during the activation of the enzyme. In the MD simulations, the lid stability was investigated by opening and closing the lid in small steps by applying restraining potentials on the pseudotorsional angles between Cα carbons in small steps. The maximum and minimum values of the pseudotorsional angles were determined from the x-ray crystal structures of the active (open) and inactive (closed) forms of Rml. Similar approaches have been used to study the bending mode of lysozyme (McCammon et al., 1976; Bruccoleri et al., 1986) and lipases (Norin et al., 1993). Previous studies of *R. miehei* lipase (Norin et al., 1993) involved either molecular mechanics minimization without MD or a combination of MD and minimization with a distance-dependent dielectric constant. In the present study we have extended the previous investigation, first to explore the effects of different dielectric models (constant and distance-dependent dielectric constant) on the restrained opening of the lid. Dielectric constant values of $\epsilon = 4$, 8, and 12 were used in the MD simulations, and values ranging from 4 to 80 were used in the BD simulations. The relatively low values were chosen because it is expected that the mobility of the water is greatly reduced in the vicinity of the lipid interface, and hence, the partially fixed water dipoles near the interface lead to a reduced dielectric constant of water in this region. The effective dielectric constant of water is estimated to be $\epsilon \approx 5$ in the vicinity of methyl ester monolayers (Vogel and Möbius, 1988); $\epsilon = 6-8$ near polar monolayer headgroups (Demchak and Fort, 1974), $\epsilon = 14-21$ near zeolite surfaces (Foster and Resing, 1976); and $\epsilon = 36-41$ near micelle interfaces (Mukerjee et al., 1977).

Second, we have carried out BD simulations to study the dynamics of the helical loop, and in particular, to address the following: 1) What is the time scale for opening of the lid? 2) Does the loop act as a gate opening and closing over the active site in hydrophilic or hydrophobic environments? and 3) Does the loop (partially) unfold during activation of the enzyme? In a recent study (Norin et al., 1994), the structural properties of Rml in water and nonpolar solvent (methyl hexanoate) were investigated. Although partial opening of the lid was only observed in nonpolar solvent, these simulations were only performed on a short time scale (200 ps). Motions of peptide loops occur on time scales of 10^{-9} to 10^{-1} s (Wade et al., 1993; Kempner, 1993; Philippopoulos et al., 1995; Falzone et al., 1994; Williams and McDermott, 1995), which, at the present time, are not accessible with standard MD techniques, when the protein is modeled in full atomic detail. We have therefore utilized a BD technique, which has been used for studying the motion of a loop over the active site of triose phosphate isomerase (Wade et al., 1993, 1994), in which the amino acid residues in the loop are represented by suitably parameterized spheres undergoing diffusive motion and the remaining part of the protein is held fixed.

Our presentation is organized as follows. In the next section, the potential model and simulation details are described. We then present our results and finally, the main findings of our investigation are summarized.

MODEL AND SIMULATION DETAILS

The conformational change occurring during the activation of Rml was simulated by MD and BD. An essential consideration is the influence of the lipid substrate on the activation pathway and dynamics. To elucidate the effect of a hydrophobic environment, we approximated the lipid substrate by a simple continuum medium surrounding the enzyme and examined the effect of variation of its properties on the motions of the active site lid.

Molecular dynamics

High-resolution crystal structures of the native Rml resolved to 1.9 Å (Z. Derewenda et al., 1992), and those of a lipase inhibitor complex resolved to 2.6 Å (Brzozowski et al., 1991) were used as models for the inactive and active structures, respectively. Both structures were obtained from

the Protein Data Bank at Brookhaven (Bernstein et al., 1977). The entry codes are 3tgl and 4tgl for the inactive and active lipases, respectively. The structures reveal that the conformational change observed during activation is restricted to 23 residues of the total of 269 and can be described as hinge bending of the helical loop covering the active site.

Polar hydrogen atom coordinates were generated, and simulations were carried out using the CHARMm polar atom force field (Molecular Simulations, 1992). All of the atoms that define the lid region (residues 76–98) and all atoms in the side chains of all of the residues within a distance of 6 Å from any atom in residues 76–98 in the initial structures of the active and inactive lipases were allowed to move. In the MD simulations, the conformational change was simulated by restraining the Cα pseudotorsional angles with a harmonic function with a force constant of 1000 kcal/mol/rad^2 to move the lid between the inactive and active forms of Rml in 20 steps. To determine the pseudotorsional angles of the inactive and active forms, each structure was optimized by applying 200 steps of steepest-descent energy minimization followed by 600 steps of conjugate gradient energy minimization. In the simulations, two different minimization schemes were used to test the sensitivity of the methodology. In the first approach (hereafter called M1), the pseudotorsional constraints were released before performing energy minimization, and only the active atoms defined above were minimized. In the second approach (hereafter called M2), the backbone atoms of those side chains that were part of the dynamic region were also included in the minimization. Throughout the simulations, a time step of 1 fs was used. The nonbonded pair list was updated every 10 fs, and the potential was truncated at 15 Å. The SHAKE algorithm (Ryckaert et al., 1977) was applied to constrain the bond lengths to their equilibrium positions, and the equations of motion were solved using the Verlet algorithm (Allen and Tildesley, 1989). The simulation was started from the minimized inactive closed structure of Rml, which initially was slowly annealed by increasing the temperature by 5°C every 50 time steps up to a temperature of 300 K. This period was followed by an additional equilibration phase of 3 ps. The annealed and equilibrated structure was used as the starting conformation for the next simulation, in which a new set of pseudotorsional angles was applied to enforce the opening of the lid. Energies were sampled every 0.05 ps over a simulation period of 5 ps. This scheme was used sequentially for all sets of pseudotorsional angles, leading, at the 20th step, to the active lipase structure. The calculations were performed both in the forward (opening) and backward (closing) directions. After each run, the structure was minimized, using 200 steps of steepest-descent energy minimization followed by 600 steps of conjugate gradient energy minimization. Several simulations were carried out, using different values for the dielectric constant, which was either taken to be a constant (CDIE; $\epsilon = \epsilon_C$) or a distance-dependent (RDIE; $\epsilon = \epsilon_C r$) quantity. $\epsilon = \epsilon_C r$ acts as an approximate solvent screening term in which the electrostatic interaction between two charges experiences greater attenuation as they are separated.

Brownian dynamics

The crystal structure of the inactive form of Rml (3tgl) was used for the BD simulations. Polar hydrogen atoms were added to the crystal structure using the CHARMm program in the QUANTA software package (Molecular Simulations, 1992). All titratable residues were assumed to adopt their usual protonation state at neutral pH, and the tautomeric state of histidine residues was assigned by graphical analysis of their hydrogen bond geometries. The positions of the added hydrogen atoms were optimized while keeping the other atoms fixed by means of energy minimization (100 steps steepest descent), brief (0.3 ps) heating to 300 K with molecular dynamics, and further energy minimization (200 steps steepest descent).

The electrostatic potential of the protein was calculated by solving the finite-difference linearized Poisson-Boltzmann equation using the incomplete Choleski conjugate gradient method (Davis et al., 1990; Davis and McCammon, 1989, 1991; Northrup et al., 1982, 1984; McCammon and Northrup, 1981) at a range of solvent dielectric constants. The protein dielectric constant was set to 2. The atoms of the protein were assigned point charges and radii (equal to $2^{(-5/6)}\sigma$; this makes the model of the solute consistent with the spherical probe model of a water molecule used to define the solvent-accessible surface; Lee and Richards, 1971) from the optimized potentials for liquid simulations (Jorgensen and Tirado-Rives, 1988) parameter set. The radii of hydrogen atoms were set to zero, and the molecular surface was calculated with a probe of radius 1 Å (Lee and Richards, 1971; Janin, 1979; Richmond and Richards, 1978; Chothia, 1976). This probe radius, when used with the above solute atom radii, gives a description of the solvent-accessible surface that is consistent with observations of water molecules in protein cavities (Wierenga et al., 1991, 1992). The relative dielectric constant was "smoothed" at the molecular surface, so that it changed gradually between the protein and solvent values (Davis and McCammon, 1991). The protein was assumed to be surrounded by aqueous solution of 0.1 M ionic strength with the ion density having a Boltzmann distribution at 300 K and excluded from a 2-Å-thick Stern layer on the protein surface.

The potential was first calculated on a 65 × 65 × 65 grid with a 2.5-Å spacing centered on the protein, using boundary conditions at the edges of the grid for which each atom is considered as a Debye Hückel sphere. A second "focused" potential was then calculated using a 65 × 65 × 65 grid with a 1.0-Å spacing and boundary conditions assigned from the first potential. This potential was used to calculate the electrostatic forces during the BD simulations. For the BD simulations, the electrostatic potential was calculated only for the part of the protein that was held fixed, i.e., the

mobile lid residues were omitted. During the simulation, the lid residues moved in the electrostatic field of the fixed atoms of the protein.

The peptide "lid" was modeled as a linear chain of spheres in which each residue was represented by a single appropriately parameterized sphere initially centered on its Cβ atom. The chain consisted of 18 residues (80–97), the central 12 residues (83–94) of which were allowed to move. The three residues at each end were held fixed but contributed to the forces on the mobile residues. The spheres were linked by pseudobonds, the lengths of which were maintained by geometric constraints (Luty et al., 1993). All of the spheres were assigned identical hydrodynamic radii of 3.15 Å. Hydrodynamic interactions between the loop residues were neglected. A central point charge was assigned to each residue corresponding to its overall charge.

The motion of each residue was determined by forces due to the other residues and due to the fixed atoms in the protein. The forces due to other mobile residues were calculated according to a modified (Wade et al., 1993; McCammon et al., 1980) version of the model of Levitt and Warshel (Levitt and Warshel, 1975; Levitt, 1976). They consisted of angle and torsional forces to model the peptide geometry, a helix stabilization force, an excluded volume force to prevent van der Waals overlaps, a solvent interaction force to model the propensity of different residues to associate in water, and electrostatic forces.

The force field was as used previously (Wade et al., 1993) except for the following modifications:

- Residue-specific parameters were used for the excluded volume and solvent interaction terms. Parameters for the excluded volume term were from set B in table 4 of Levitt and Warshel (1975), and parameters for the solvent interaction term were from table 3 of Levitt and Warshel (1975).
- Solvent interaction terms were calculated between mobile residues and fixed atoms of the protein.
- A helix stabilization term was calculated according to the method of McCammon et al. (1980). The residues for which this term may be calculated were defined, for this lipase, as residues 84–92. The helix stabilization term was a function of the dihedral angles between subunits and was only calculated for dihedral angles in the range 25–55°C; otherwise it was set to zero. The stabilization energy was smaller for the terminal residues (up to 1.4 kcal/mol) than for the interior residues (up to 6 kcal/mol). The stabilization energies were chosen to approximately reproduce the experimental Zimm-Bragg s parameter for valine describing its helix-forming propensity (McCammon et al., 1980). Simulations were done with two helix definitions. In the first (hereafter called cran for constant range), the length of the helix and the positions of its terminii were constant. According to this definition, the helix could unwind, resulting in zero stabilization energy, but the same residues were always defined as terminal ones. For the second helix definition (hereafter referred to as vran for variable range), the length of the helix and the identities of the terminal residues could vary according to the values of the dihedral angles. The helix could also break into more than one helix, each with its own terminal residues.

Each mobile residue was subjected to electrostatic and solvent interaction forces from the fixed atoms of the protein. Penetration of the mobile residues into the volume of the fixed atoms in the protein was prevented by making corrections at each step. The excluded volume of the fixed atoms was defined by the surface of a 2-Å-radius sphere rolled over the fixed atoms assigned standard OPLS radii (σ and nonzero hydrogen radii). If, when moved, a residue would fall within the excluded volume of the fixed atoms, that residue was returned to its original position and the pseudobonds in the moving loop were reconstrained. Overlaps between the moving residues and the fixed atoms were checked again, and if present, the correction procedure was repeated. This was continued until there were no unfavorable close contacts between the moving residues and the fixed atoms or until five cycles of movements and reconstraints had been performed. In the latter case, the new positions of the residues that satisfied the excluded volume criteria were used regardless of whether the bond constraints were satisfied. The solvent interaction term was calculated from the distance of the C_β atom of each fixed residue, using residue-specific parameters.

The motion of the lid was modeled with parameters set to simulate surroundings varying from aqueous polar to nonpolar. Aqueous solution was modeled with a high dielectric constant and the solvent interaction term. Nonpolar surroundings were modeled by using a low dielectric constant and not calculating the solvent interaction term. The solvent interaction term is parameterized to model the probability of bringing two residues together in aqueous solution. Therefore, a simple model of this probability in nonpolar solution is achieved by removing it. Trajectories were generated using the Ermak-McCammon equation (Ermak and McCammon, 1978). The protein was assigned a radius of 29 Å, and a time step of 0.01 ps was used. All electrostatic and BD calculations were performed with a modified version of the UHBD program, version 4.1 (Davis et al., 1990; Madura et al., 1995) on Silicon Graphics workstations.

RESULTS AND DISCUSSION

Molecular dynamics

Constrained MD simulations were performed using a constant (CDIE) or a distance-dependent (RDIE) dielectric constant. Conformational changes were simulated by adding a pseudotorsional potential to the force field, which enforces the movement of the lid between the inactive and active structures. Fig. 1 displays the inactive and active conformations of the Rml. The lid region is indicated by the light grey color, where the cylinders represent the helical lids of the inactive form (lower position) and the active form (upper position). The reliability of this method can be tested by closing as well as opening the lid. The process should be

reversible, i.e., in terms of energy and structural root-mean-square displacement (rmsd) the differences between simulated and crystal structures should be small. A typical example is shown in Fig. 2 for $\epsilon = 8$ using CDIE and RDIE. In the simulations using CDIE, two different minimization schemes were used to test the sensitivity of the methodology. The results are displayed in Fig. 3, where the mean energy differences, $E_{active} - E_{inactive}$, are plotted as a function of dielectric constant. E_{active} and $E_{inactive}$ refer to the total energy (i.e., potential energy) of the active and inactive forms, respectively. $E_{inactive}$ is an average value calculated from the energies determined before restrained opening and after restrained opening and closing. For $\epsilon = 8$, we observe that the two schemes (CDIE and RDIE) yield similar results. Larger deviations are found for lower dielectric constants. No reliable data were obtained for $\epsilon = 2$, because in this low dielectric constant medium, ARG86 and ASP91 form a salt bridge, which causes a large displacement of ARG86 from its position in the inactive crystal structure. The calculated energy difference between the inactive and active structures

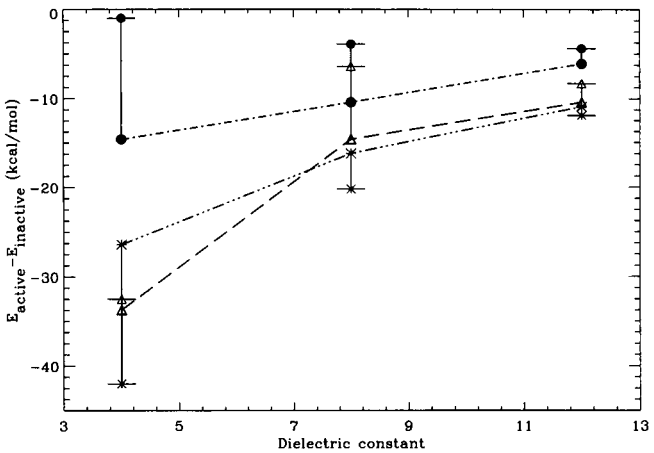

FIGURE 3 The mean energy difference between the active and the inactive Rml structures as a function of dielectric constant. ●, CDIE with minimization scheme M1; *, CDIE with minimization scheme M2; △, RDIE with minimization scheme M2. For both dielectric treatments the open form is more stable. Error bars (half shown) are estimated from the difference in $E_{inactive}$ calculated before and after opening and closing the lid.

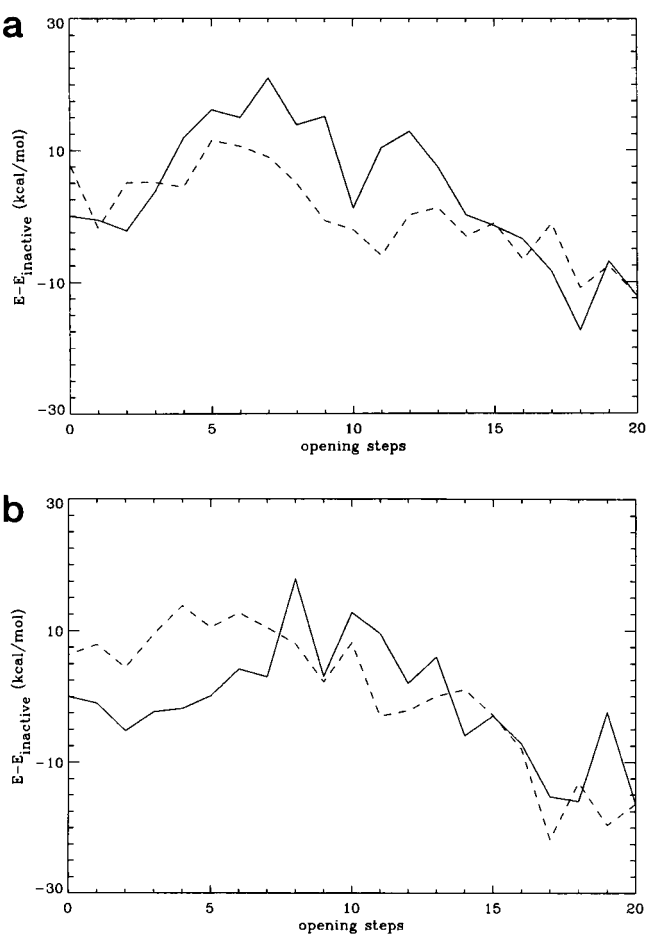

FIGURE 2 Total energy difference, $E - E_{inactive}$, between simulated structures and the inactive Rml structure calculated during the MD simulations of a restrained change in the lid conformation. Results are shown for model (M2) using (*a*) CDIE = $\epsilon = 8$ and (*b*) RDIE = $\epsilon \cdot \gamma = 8 \cdot \gamma$. Lines correspond to opening (——) and closing (– – –).

depends on the choice of the movable part of the enzyme and the protocol for simulation and minimization. Scheme M2 results in lower energy values than scheme M1, indicating that more strain between the movable and fixed parts of the enzyme is released. Although similar results were obtained for the simulations using CDIE and RDIE, the energies recorded during opening and closing were smoother for the RDIE methodology at a lower dielectric constant, which is reflected in the error bars shown in Fig. 3. However, the results of the different approaches follow the same trend; it is energetically favorable for the enzyme to become active in a low dielectric environment, where strong electrostatic interactions lead to stabilization of the active conformer.

Brownian dynamics

In the previous model, pseudotorsional constraints were applied to reduce the computational burden. A shortcoming of this approximation is the biasing of the activation pathway toward the pathway defined by the restraints and the lack of information about the dynamical properties of the loop along the pathway between inactive and active forms. Loop motions that occur on time scales of nanoseconds or longer are too expensive to study by MD. We therefore utilized BD to investigate the motion of the lid under different environmental conditions and periods up to 1 μs. In these simulations, the motion of the loop residues is governed by electrostatic, solvent interaction, and excluded volume forces from the stationary part of the protein, the forces due to the other mobile residues, and the random frictional forces due to solvent. We maintained the approximation that the surrounding environment is modeled as a continuum. It is characterized by two parameters: ϵ and the

presence or absence of a solvent interaction force. These parameters were varied to elucidate their effect of these parameters on the activation of Rml. A summary of the simulation details is provided in Table 1, and representative images of distinct lid conformations are displayed in Fig. 4, *a–f*.

$\epsilon = 80$ versus $\epsilon = 4$

Simulation results obtained for $\epsilon = 80$ and 4 are shown in Figs. 4–7. The primary quantities computed in the simulations are the rmsd calculated between the crystal structure of the inactive form and the structures obtained during the course of the simulations and distances between certain charged residues. The rmsd data were calculated between the simulated structure at time t and the crystal structure of the inactive form using the coordinates for the Cβ atoms, or in the case of Gly, the Cα atom. All data were normalized by the number of mobile residues. The rmsd calculated between the active and inactive crystal structures is 2.5 Å. To define an opening time, we have used the criterion that the rmsd should be larger than 2.2 Å for at least 50 ns. Reported times are taken at the beginning of this 50 ns. The time evolution of the rmsd is shown in Fig. 5 for $\epsilon = 4$ and $\epsilon = 80$. Simulations were performed without solvent interaction between flexible loop and fixed protein atoms, and intralid solvent interaction was only included at high dielectric constant. A characteristic feature of all of these runs is that after opening or partial opening of the lid, only small fluctuations in the rmsd data are observed at low and high dielectric constant values. The effect of solvent on the activation of Rml will be discussed below (see Effect of Mutation). Conformations of the lid observed in the simulations at $\epsilon = 80$ and $\epsilon = 4$ are shown in Fig. 4, *a* and *b*, respectively. At $\epsilon = 80$, the lipase lid is partially open, whereas at $\epsilon = 4$, it appears that the simulated structure is slightly more open than shown by the crystal structure of the active lipase. Deviations of open simulated structures from the crystal structure of the Rml-inhibitor complex (active form) may be caused by several effects. They may be due to the simplicity of the model, but a direct comparison of the structures is difficult, because the active conformation was taken from the crystal structure of a lipase inhibitor complex, where the actual position of the lid is probably influenced by the inhibitor and by crystal contacts (Derewenda, 1995).

ϵ dependence

As the dielectric constant of the medium is increased, the opening time of the lid is increased and the stability of the open form decreases, i.e., opening is only partial and the open structure undergoes large fluctuations. Opening times determined from the rmsd are given in Table 1. The estimated errors in the opening times are considerable, and it would require a large number of simulations to calculate precise opening times. However, the dependence of the opening time on the dielectric constant fits the general view of the function of lipases, which undergo a tremendous increase in activity when the substrate concentration exceeds the critical micelle concentration for the substrate, indicating that the presence of a lipid interface improves the activation of lipases and hence the opening time increases many-fold with increasing dielectric constant (ϵ). Our results indicate that the helical lid does not fully open at $\epsilon = 80$, and a much lower dielectric constant medium such as the lipid interface is required for the lipase to open fully to

TABLE 1 Simulation details of the Brownian dynamics

Dielectric constant	Lid intrasolvent interaction	Lid-protein solvent interaction	Helix treatment	Sequence	Simulation time period (ns)	Opening time (ns)	Fig.
4	−	−	cran	wt	900,300,300,300,300 300,300,300	94 ± 79	4 *b* 4 *d* and *e*
4	−	−	vran	wt	300,300,300,300,300	84 ± 63	4 *d* and *e*
4	+	−	cran	wt	300	100	−
12	−	−	cran	wt	900,300	95 ± 50	−
12	−	+	cran	wt	100,100,300,300	90 ± 57	−
28	−	−	cran	wt	900	140	−
36	−	−	cran	wt	900,600	298 ± 202	−
36	−	+	cran	wt	300	>300	−
44	+	−	cran	wt	900	75	−
52	+	−	cran	wt	900	155	−
66	+	−	cran	wt	900	130	−
66	+	+	cran	wt	300	>300	−
73	+	+	cran	wt	300	>300	−
80	−	−	cran	wt	900,900	270 ± 156	−
80	+	−	cran	wt	900,600,900	300 ± 57	4 *a*
80	+	+	cran	wt	600,600,900	>624 ± 265	4 *c*
4	−	−	cran	ARGN86	500	>500	4 *f*
4	−	−	cran	ASPH91	500	230	−
4	−	−	cran	ARGN86-ASPH91	500	>500	4 *f*

+ and − refer to the presence and absence of solvent interaction forces, respectively.

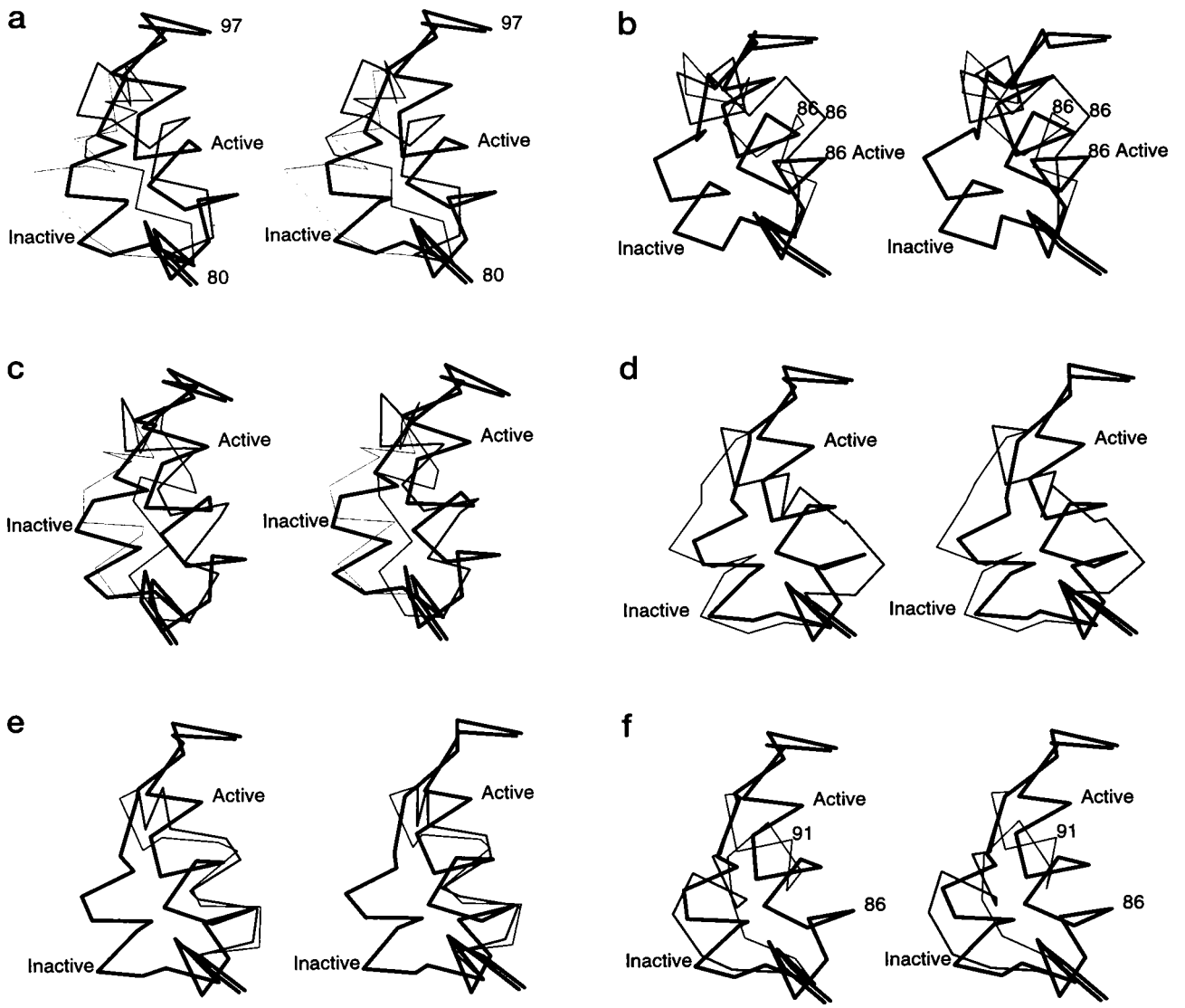

FIGURE 4 Stero views of the conformation of the active site lid in the crystal structures of the open and closed forms of Rml (bold) and at times during the BD simulations (increasing thickness corresponds to increasing time). (*a*) $\epsilon = 80$; snapshots at 50, 200, and 600 ns; with intralid solvent interaction. (*b*) $\epsilon = 4$; snapshots at 50 and 300 ns; without intralid solvent interaction. (*c*) $\epsilon = 80$; snapshots at 20, 120, and 220 ns; with intralid solvent and lid-protein solvent interactions. (*d*) $\epsilon = 4$; using fixed (thin line; cran) or variable (thick line; vran) helix length. Snapshots were taken at 117 ns; without solvent interactions. (*e*) $\epsilon = 4$; snapshots at 300 ns; see *d* for more details. (*f*) $\epsilon = 4$; snapshots at 300 ns; for ARGN86 (thin line) and ARGN86-ASPH91 (thick line); without solvent interactions.

give access to the substrate. This reflects the importance of electrostatic interactions between charged amino acid groups. This is also observed from the time evolution of the distances between the charged residues in the lid (ARG86 and ASP91) and those close to the lid (ASP61, ASP113, and ASP203), which are displayed in Figs. 6 and 7 for $\epsilon = 80$ and $\epsilon = 4$, respectively. The corresponding distances observed in crystal structures of the inactive and active lipase forms are summarized in Fig. 8. Figs. 6 and 7 indicate that the strong electrostatic interactions between ARG86 and ASP61 as well as between ARG86 and ASP113 are important for stabilizing the open form. These interactions are weakened as the dielectric constant is increased, essentially destabilizing the active conformation of Rml. The activation of the lipase is not sensitive to the helix definition (cran versus vran). As indicated in Table 1, simulations performed with cran and vran yield similar estimates for the opening time at $\epsilon = 4$. The final open conformation of the lid is similar for both helix models (see Fig. 4 *e*). However, conformations displayed in Fig. 4 *d* suggest that when the vran option is used, the lid passes through a more unfolded state before reaching its active conformation.

Solvent interaction dependence

We performed additional runs to elucidate the effect of solvent on the activation of Rml. In these simulations, we included solvent interaction forces (which model the effect

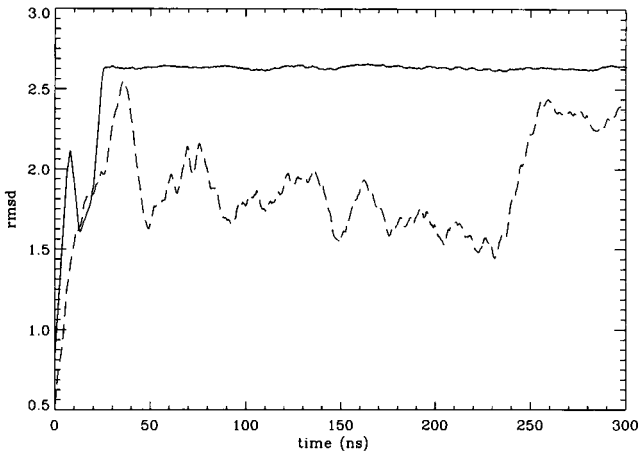

FIGURE 5 Rmsd of the Cβ positions from the crystal structure of the closed inactive conformation as a function of simulation time for simulations without lid-protein solvent interactions at $\epsilon = 4$ (——) (without intralid solvent interactions) and $\epsilon = 80$ (– – –) (with intralid solvent interactions).

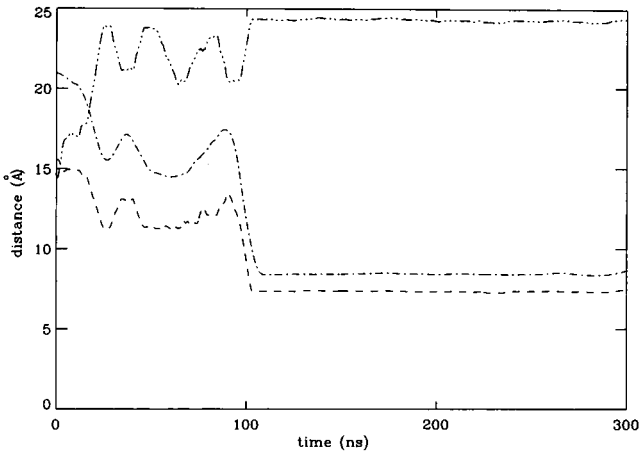

FIGURE 7 Distances between selected residues as a function of simulation time for simulations without solvent interactions. Simulations were performed at $\epsilon = 4$. The lid opens after approximately 100 ns. Line style and residue pairs are the same as in Fig. 6.

of aqueous solvent) between the flexible loop residues and the fixed protein atoms in the calculations. The time evolution of the rmsd is shown in Fig. 9. Similar opening times are observed in the simulations performed with or without solvent interaction between loop residues and fixed protein at $\epsilon = 12$ (see Table 1). These opening times are comparable with the results of the simulations performed at $\epsilon = 4$, indicating that the solvent interaction plays only a minor role at low dielectric constant. However, at high dielectric constant, this interaction becomes more important, slowing the opening of the lid. For instance, at $\epsilon = 80$, the estimated opening time is approximately 300 ns, when the lid-protein solvent interaction is excluded. Including lid-protein solvent interaction, the estimated opening time exceeded 600 ns, and in most of the runs only partial opening was observed in the simulations of up to 900 ns. Similar effects were observed at $\epsilon = 36$ and $\epsilon = 66$ (see Table 1).

Compared to the previous simulation results, where we excluded solvent interactions between loop residues and protein atoms (Fig. 5), we note that the observed fluctuations in the rmsd are much larger in a high dielectric constant medium than in a low dielectric constant medium, and no reliable opening time could be estimated. The extent of the fluctuations is an indication that the loop motion is substantially influenced by an aqueous environment in which electrostatic interactions between charged residues in

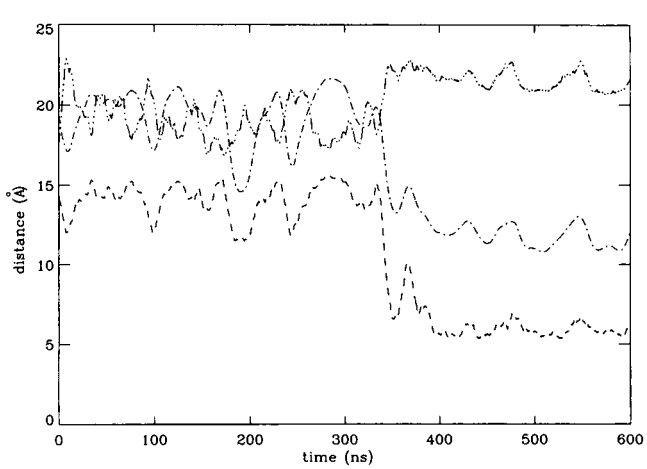

FIGURE 6 Distances between selected residues as a function of simulation time for simulations with intralid solvent interactions, but without lid-protein solvent interactions. Distances are given for ARG86-ASP61 (– – –), ARG86-ASP113 (– · — · —), and ARG86-ASP203 (– ··· –). Simulations were performed at $\epsilon = 80$. The lid opens after approximately 300 ns.

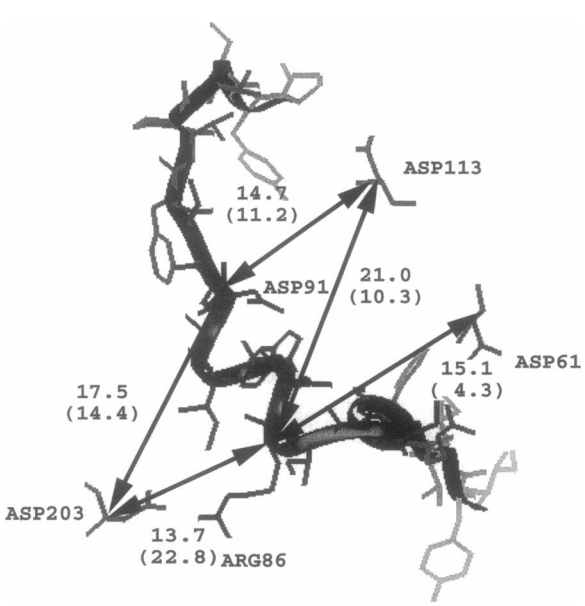

FIGURE 8 Selected distances between key residues determined from the crystal structures of the inactive and active enzyme. Only the structure of the inactive form is shown. Numbers in parantheses refer to the active conformation. Data are given in angstroms.

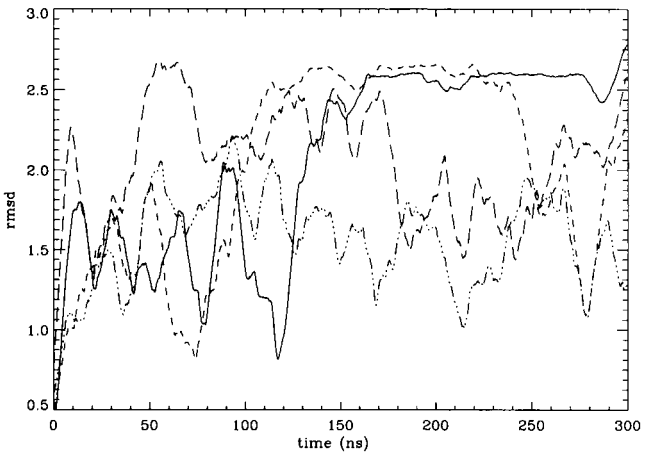

FIGURE 9 Rmsd of the Cβ positions from the crystal structure of the closed conformation as a function of simulation time for simulations at ϵ = 4 (——) (without solvent interactions), 12 (- - -), (without solvent interactions), 36 (– ··· –) (with lid-protein solvent interaction), and 80 (– – –) (with intralid and lid-protein solvent interactions).

the lid region are screened, and it is the interplay between these two contributions (hydrophilicity/hydrophobicity and electrostatics) that determines the activation of the lipase. Stereo views of distinct conformations taken at ϵ = 80 are shown in Fig. 4 *c*. Visualization of snapshots indicates that the loop fluctuates around the conformations corresponding to 120 and 220 ns. It is important to note that Fig. 4 *c* displays the two extreme conformations observed during the fluctuations of the lid, whereas Fig. 4 *a* displays lid configuration as a function of simulation time (i.e., the continuous opening of the lid). To further investigate the nature of the coulombic interactions, we have analyzed the electrostatic forces on the residues ARG86 and ASP91. The time evolution of the forces is shown in Figs. 10 and 11 for ϵ = 4 and ϵ = 80, respectively. A noticeable difference is observed between the forces. The force on residue ARG86 is approximately twice that on ASP91 at ϵ = 4. As the dielectric

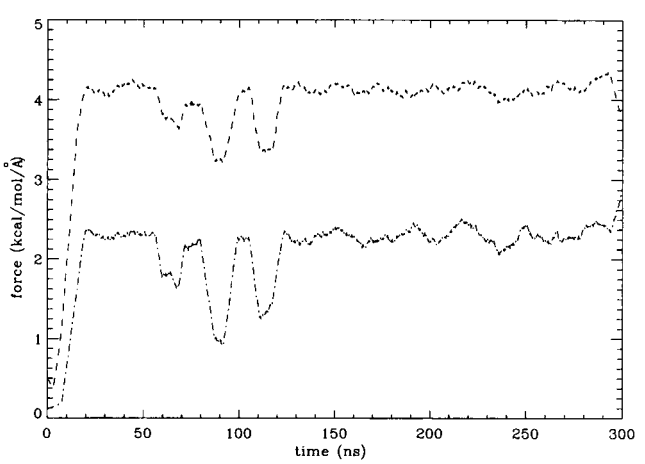

FIGURE 10 Electrostatic force on residues ARG86 (– – –) and ASP91 (– · – · –) for simulations without solvent interactions at ϵ = 4.

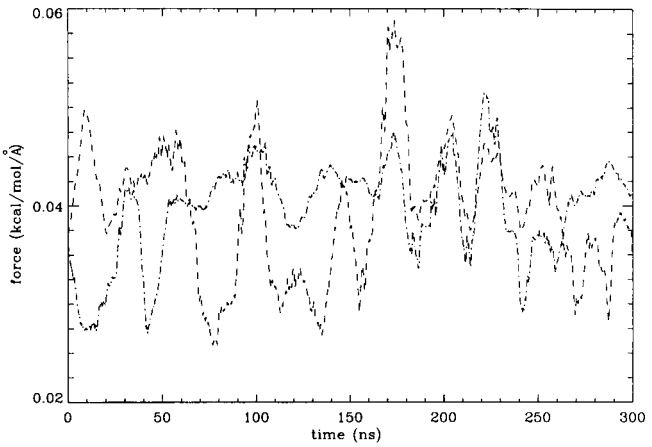

FIGURE 11 Electrostatic force on residues ARG86 (– – –) and ASP91 (– · – · –) for simulations with intralid and lid-protein solvent interactions at ϵ = 80.

constant is increased to ϵ = 80, the forces become equal in magnitude and decrease by a factor of approximately 100. As observed earlier, at low dielectric constant, the electrostatic interactions are strong enough to stabilize the active conformation of Rml, whereas in an aqueous solution, these forces are screened and usually result in a partially open structure.

Effect of mutation

MD and BD results show that electrostatics is a key parameter in the activation of Rml. To further elucidate the importance of ARG86 and ASP91 in the mechanism, we have conducted additional simulations in which these two residues were mutated to neutral groups (ARGN86 and ASPH91, respectively). As indicated in Table 1, mutations ARGN86, ASPH91, and ARGN86-ASPH91 were considered. In the simulation with the mutant (ARGN86 and ASPH91), the electrostatic interactions of the loop are absent, because there are only two charged residues in the loop. Fig. 12, *a* and *b*, shows the time evolution of the distances between ARGN86 and aspartic acid residues 61, 113, and 203, which were monitored during the simulation with the mutant ARGN86. Loop configurations observed during the simulations with mutants ARGN86 and ARGN86-ASPH91 are displayed in Fig. 4 *f*. In both simulations, the loop remains close to the inactive conformation but is partially unfolded, suggesting that both charged groups contribute to the stabilization of the helical loop. It is interesting to note that in the simulation with ARGN86, the negatively charged ASP91 is pulled over to the active conformation, which could indicate that repulsive forces acting on ASP91 in the inactive form and attractive forces between ARG86 and ASP61 as well as ASP113 enhance the lipase activation. Simulations performed with a mutant where only ASP91 has been mutated to ASPH91 result in an active conformation. The observed opening time is on the same order as for the native Rml, indicating that the role of ARG86 in the activation of Rml is more important than

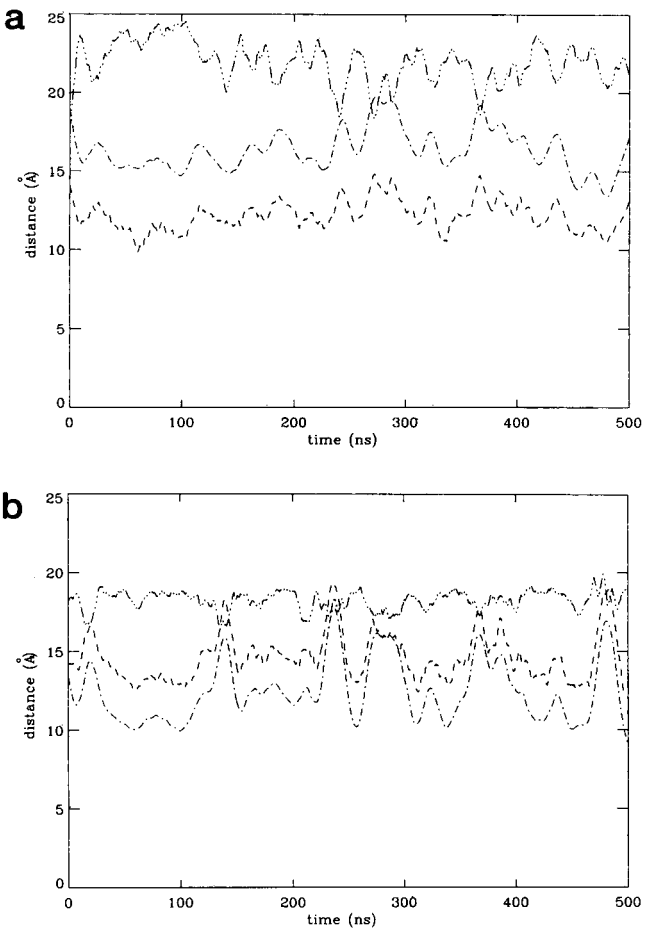

FIGURE 12 ASP113 and ASP203 and (*b*) ASP91 and ASP61, ASP113, and ASP203 as a function of simulation time at $\epsilon = 4$ (without solvent interactions). ARG86 is mutated to ARGN86. Line style in *a* is the same as in Fig. 6. (*b*) Distances are given for ASP91-ASP61 (– – –), ASP91-ASP113 (– · – · –), and ASP91-ASP203 (– ·· – ·· –). The lid does not open.

ASP91. The importance of ARG residues, and in particular ARG86, is shown by experiments in which enzyme activity is reduced when they are chemically modified. It is observed that guanidine can competitively inhibit the activation of Rml. This is thought to be because guanidine is chemically analogous to the end of an ARG side chain, and therefore competes with ARG86 for hydrogen-bonding partners. When assayed on tributyrin substrate, Rml showed approximately one-third of its normal activity in the presence of guanidine. The inhibition is not observed in Rml, when guanidine was added after the addition of substrate, suggesting that the ARG in Rml is only important during the activation process (Holmquist et al., 1993).

CONCLUSION

In conclusion, we have investigated the activation of Rml under different environmental conditions using MD and BD. Restrained MD was applied to estimate the energy gain during activation, whereas BD was employed to estimate the time scale of opening and elucidate the loop dynamics upon activation of the enzyme. The time scale for opening is approximately 100 ns in a lipid-like environment. In an aqueous solution, the lid opens more slowly and exhibits gating of the active site. To study some of the effects of a lipid interface on the activation of the enzyme, we have approximated the substrate by a continuum model using different values of the dielectric constant and a solvation interaction term. Both constrained MD and BD suggest that the enzyme activity increases as the surrounding medium's dielectric constant is lowered, and the active form is stabilized by electrostatic interactions between charged residues. Key residues are ARG86 and ASP91 in the lid region and ASP61 and ASP103 close to the lid in the open conformation. Mutation of ARG86 and ASP91 to neutral amino acid groups reveals that, in the closed conformation, ASP91 pushes the lid toward the open conformation, whereas ARG86 forms a salt bridge with ASP61 in the active open form. As the dielectric constant increases, this interaction is screened and hence the active form is destabilized. Mutation of both ARG86 and ASP91 to neutral residues results in a closed conformation of Rml and the loop unfolds, suggesting that interactions between ARG86 and ASP91 contribute to the stabilization of the helical structure of the loop. Changing the properties of the loop by using cran (constant length of the helix and positions of its terminii) and vran (variable length of the helix and positions of its terminii) does not change the helix structure in the open conformation, but for vran the helix goes through a more unfolded state during activation. These simulations indicate the important role for salt links in controlling lipase activation, which could be investigated in site-directed mutagenesis experiments. They also suggest that engineering of additional salt links could lead to increased activity.

Computations were performed at Novo-Nordisk A/S.

GHP would like to acknowledge financial support from the European grant BIOZ-CT93-5507.

REFERENCES

Allen, M. P., and D. J. Tildesley. 1989. Computer Simulation of Liquids. Clarendon, Oxford.

Bernstein, F. C., T. F. Koetzle, G. J. B. Williams, E. F. Meyer, M. D. Brice, J. R. Rogers, O. Kennard, T. Shimanouchi, and M. Tasumi. 1977. The Protein Data Bank: a computer based archival file for macromolecular structure. *J. Mol. Biol.* 112:535–542.

Brockman, H. L. 1984. Lipases. B. Bergström and H. L. Brockman, editors. Elsevier Science Publishers, Amsterdam. 1–46.

Bruccoleri, R. E., M. Karplus, and J. A. McCammon. 1986. The hinge-bending mode of a lysozyme-inhibitor complex. *Biopolymers.* 25: 1767–1802.

Brzozowski, A. M., U. Derewenda, Z. S. Derewenda, G. G. Dodson, D. M. Lawson, J. P. Turkenburg, F. Bjorkling, B. Huge-Jensen, S. A. Patkar, and L. Thim. 1991. A model for interfacial activation in lipases from the structure of a fungal lipase-inhibitor complex. *Nature.* 351:491–494.

Chothia, C. 1976. The nature of the accessible and buried surfaces in proteins. *J. Mol. Biol.* 105:1–14.

Davis, M. E., J. D. Madura, B. A. Luty, and J. A. McCammon. 1990. Electrostatics and diffusion of molecules in solution: simulations with

the University of Houston Brownian dynamics program. *Computer Physics Communications.* 62:187–197.

Davis, M. E., and J. A. McCammon. 1989. Solving the finite difference linearized Poisson-Boltzmann equation: a comparison of relaxation and conjugate gradient methods. *J. Comput. Chem.* 10:386–391.

Davis, M. E., and J. A. McCammon. 1991. Dielectric boundary smoothing in finite difference solutions of the Poisson equation: an approach to improve accuracy and convergence. *J. Comput. Chem.* 7:909–912.

Demchak, R. J., and T. Fort Jr. 1974. Surface dipole moments of close-packed un-ionized monolayers at the air-water interface. *J. Colloid Interface Sci.* 46:191–202.

Derewenda, U., A. M. Brzozowski, D. M. Lawson, and S. Z. Derewenda. 1992. Catalysis at the interface: the anatomy of a conformational change in a triglyceride lipase. *Biochemistry.* 31:1532–1541.

Derewenda, U., L. Swenson, Y. Wei, R. Green, P. M. Kobos, R. Joerger, M. J. Haas, and Z. S. Derewenda. 1994. Conformational lability of lipases observed in the absence of an oil-water interface: crystallographic studies of enzymes from the fungi *Humicola lanuginosa* and *Rhizopus delemar. J. Lipid. Res.* 35:524–534.

Derewenda, Z. S. 1995. A twist in the tale of lipolytic enzymes. *Nature Struct. Biol.* 2:347–349.

Derewenda, Z. S., U. Derewenda, and G. G. Dodson. 1992. The crystal and molecular structure of the *Rhizomucor miehei* triacylglyceride lipase at 1.9 angstroms resolution. *J. Mol. Biol.* 227:818–839.

Ermak, D. L., and J. A. McCammon. 1978. Brownian dynamics with hydrodynamic interactions. *J. Chem. Phys.* 69:1352–1360.

Falzone, C. J., P. E. Wright, and S. J. Benkovic. 1994. Dynamics of a flexible loop in dihydrofolate reductase from *Escherichia coli* and its implication for catalysis. *Biochemistry.* 33:439–442.

Foster, K. R., and H. A. Resing. 1976. The low apparent permittivity of adsorbed water in synthetic zeolites. *J. Chem. Phys.* 80:1390–1392.

Holmquist, M., M. Norin, and K. Hult. 1993. The role of arginines in stabilizing the active open-lid conformation of *Rhizomucor miehei* lipase. *Lipids.* 28:721–726.

Janin, J. 1979. Surface and side volumes in globular proteins. *Nature.* 277:491–492.

Jorgensen, W. L., and J. Tirado-Rives. 1988. The OPLS potential functions for proteins. Energy minimizations for crystals of cyclic peptides and crambin. *J. Am. Chem. Soc.* 110:1657–1666.

Kempner, E. S. 1993. Movable lobes and flexible loops in proteins. Structural deformations that control biochemical activity. *FEBS Lett.* 326:4–10.

Lee, B., and F. M. Richards. 1971. The interpretation of protein structures: estimation of static accessibility. *J. Mol. Biol.* 119:379–400.

Levitt, M. 1976. A simplified representation of protein conformations for rapid simulation of protein folding. *J. Mol. Biol.* 104:59–107.

Levitt, M., and A. Warshel. 1975. Computer simulation of protein folding. *Nature.* 253:694–698.

Luty, B. A., R. C. Wade, J. D. Madura, M. E. Davis, J. M. Briggs, and J. A. McCammon. 1993. Brownian dynamics simulations of diffusional encounters between triose phosphate isomerase and glyceraldehyde phosphate: electrostatic steering of glyceraldehyde phosphate. *J. Phys. Chem.* 97:233–237.

Madura, J. D., J. M. Briggs, R. C. Wade, M. E. Davis, B. A. Luty, A. Ilin, J. Antosiewicz, M. K. Gilson, B. Bagheri, L. R. Scott, and J. A. McCammon. 1995. Electrostatics, and diffusion of molecules in solution: simulations with the University of Houston Brownian dynamics program. *Computer Physics Communications.* 91:57–95.

McCammon, J. A., B. R. Gelin, M. Karplus, and P. G. Wolynes. 1976. The hinge-bending mode of lysozyme. *Nature.* 262:325–326.

McCammon, J. A., and S. H. Northrup. 1981. Gated binding of ligands to proteins. *Nature.* 293:316–317.

McCammon, J. A., S. H. Northrup, M. Karplus, and R. M. Levy. 1980. Helix-coil transitions in a simple polypeptide model. *Biopolymers.* 19: 2033–2045.

Molecular Simulations. 1992. CHARMm Molecular Modeling Software Package, Release 3.3. Molecular Simulations, Waltham, MA.

Muderhwa, J. M., and H. L. Brockman. 1992. Lateral lipid distribution as a major regulator of lipase activity. *J. Biol. Chem.* 267:24184–24192.

Mukerjee, P., J. R. Cardinal, and N. R. Desai. 1977. *In* Micellization, Solubilization and Mikroemulsion. K. Mittal, editor. New York. 249.

Norin, M., F. Haeffner, K. Hult, and O. Edholm. 1994. Molecular dynamics simulations of an enzyme surrounded by vacuum, water, or a hydrophobic solvent. *Biophys. J.* 67:548–559.

Norin, M., O. Olsen, A. Svendsen, O. Edholm, and K. Hult. 1993. Theoretical studies of *Rhizomucor miehei* lipase activation. *Protein Eng.* 6:855–863.

Northrup, S. H., S. A. Allinson, and J. A. McCammon. 1984. Brownian dynamics simulation of diffusion-influenced bimolecular reactions. *J. Chem. Phys.* 80:1517–1524.

Northrup, S. H., F. Zarin, and J. A. McCammon. 1982. Rate theory for gated diffusion-influenced ligand binding to proteins. *J. Phys. Chem.* 86:2314–2321.

Peters, G. H., S. Toxvaerd, N. B. Larsen, T. Bjornholm, K. Schaumburg, and K. Kjaer. 1995a. Structure and dynamics of lipid monolayers: implications for enzyme catalysed lipolysis. *Nature Struct. Biol.* 2:395–401.

Peters, G. H., S. Toxvaerd, O. H. Olsen, and A. Svendsen. 1993. Molecular dynamics computer simulations: a tool for the investigation of amphiphilic systems and enzymatic reaction mechanisms on a microscopic level. *Tenside Surf. Det.* 30:264–268.

Peters, G. H., S. Toxvaerd, O. H. Olsen, and A. Svendsen. 1995b. Modelling of complex biological systems. II. Effect of chainlength on the phase transitions observed in diglyceride monolayers. *Langmuir.* 11: 4072–4081.

Peters, G. H., S. Toxvaerd, A. Svendsen, and O. H. Olsen. 1994. Modeling of complex biological systems. I. Molecular dynamics studies of diglyceride monolayers. *J. Chem. Phys.* 100:5996–6010.

Philippopoulos, M., Y. Xiang, and C. Lim. 1995. Identifying the mechanism of protein loop closure: a molecular dynamics simulation of the *Bacillus stearothermophilus* LDH loop in solution. *Protein Eng.* 8:565–573.

Pieroni, G., Y. Gargouri, L. Sarda, and R. Verger. 1990. Interactions of lipases with lipid monolayers. Facts and questions. *Adv. Colloid Interface Sci.* 32:341–378.

Richmond, T. J., and F. M. Richards. 1978. Geometrical constraints and contact areas. *J. Mol. Biol.* 119:537–555.

Ryckaert, J.-P., G. Ciccotti, and H. J. C. Berendsen. 1977. Numerical integration of the Cartesian equations of motion of a system with constraints: molecular dynamics of *n*-alkanes. *J. Comp. Phys.* 23: 327–341.

Thuren, T. 1988. A model for the molecular mechanism of interfacial activation of phospholipase A2 supporting the substrate theory. *FEBS Lett.* 229:95–99.

Verger, R., F. Pattus, G. Pieroni, C. Riviere, F. Ferrrato, G. Leonardi, and B. Dargent. 1984. Regulation by the interfacial quality of some biological activities. *Colloids Surf.* 10:163–180.

Vogel, V., and D. Möbius, D. 1988. Hydrated polar groups in lipid monolayers: effectice local dipole moments and dielectric properties. *Thin Solid Films.* 195:73–81.

Wade, R. C., M. E. Davis, B. A. Luty, J. D. Madura, and J. A. McCammon. 1993. Gating of the active site of triose phosphate isomerase: Brownian dynamics simulations of flexible peptide loops in the enzyme. *Biophys. J.* 64:9–15.

Wade, R. C., B. A. Luty, E. Demchuk, J. D. Madura, M. E. Davies, J. M. Briggs, and J. A. McCammon. 1994. Simulation of enzyme-substrate encounter with gated actice sites. *Nature Struct. Biol.* 1:63–67.

Wierenga, R. K., M. E. Noble, and R. C. Davenport. 1992. Comparison of the refined crystal structures of liganded and unliganded chicken, yeast and trypanosomal triosephosphate isomerase. *J. Mol. Biol.* 224: 1115–1126.

Wierenga, R. K., M. E. Noble, G. Vriend, S. Nauche, and W. G. Hol. 1991. Refined 1.83 Å structure of trypanosomal triosephosphate isomerase crystallized in the presence of 2.4 M ammonium sulphate. A comparison with the structure of the trypanosomal triosephosphate isomerase-glycerol-3-phosphate complex. *J. Mol. Biol.* 220:995–1015.

Williams, J. C., and A. E. McDermott. 1995. Dynamics of the flexible loop of triosephosphate isomerase: the loop motion is not ligand gated. *Biochemistry.* 34:8309–8319.